Magnetoelectric coupling in the pyrochlore ruthenate $Gd_2Ru_2O_7$

Takuma Okamura[1], Ryuji Okazaki[1 *], Hiroki Taniguchi[1], Yukio Yasui[2], and Ichiro Terasaki[1 †]

[1]*Department of Physics, Nagoya University, Nagoya 464-8602, Japan*
[2]*Department of Physics, Meiji University, Kawasaki 214-8571, Japan*

We have prepared polycrystalline samples of $Gd_2Ru_2O_7$, and have measured the dielectric constant, magnetization and magnetostriction in external fields from 0 to 7 T below 15 K. We find that the dielectric constant of $Gd_2Ru_2O_7$ significantly changes with external fields, and reveal a finite magnetoelectric coupling in this oxide. Using a simple model in which the spins on the Gd ions feel an internal magnetic field of 7 T from the Ru clusters, we have explained magnetization and magnetoelectric effects qualitatively.

1. Introduction

In conventional response of materials to electromagnetic fields, the polarization is defined as a macroscopic field conjugate to the electric field, and the magnetization is defined as that conjugate to the magnetic field. The two macroscopic fields are basically independent, but an exceptional case is seen in the so-called magnetoelectric materials, in which there is a finite coupling between the two fields. Owing to this coupling, the polarization is proportional to the magnetic field in the absence of electric field, while the magnetization is proportional to the electric field in the absence of magnetic field.[1–3] They have been long studied over a century since Pierre Curie suggested such possibilities. In the 60's, the magnetoelectric coupling constants have been measured experimentally and calculated theoretically in Cr_2O_3.[4–7] The magnetoelectric effects have received a renewed interest since the discovery of multiferroic materials exhibiting huge response to external fields.[8–10] Recently, topologically nontrivial domain structures are observed in hexagonal multiferroic $YMnO_3$.[11] Another topologically nontrivial phenomenon is skyrmion in a multiferroic material.[12] For practical applications, $BiFeO_3$ has been extensively investigated, in which antiferromagnetic domains are controlled by electric field at room temperature.[13] Making composites of ferroelectric and magnetic materials is a practical approach to exhibit multiferroelectricity.[14]

We have searched for a new type of magnetoelectric materials.[15–17] Thus far, magnetoelectric effects have been found in magnetically ordered materials. In particular, a spiral-type magnetic order offers a necessary condition to induce ferroelectricity, because such an order breaks time-reversal symmetry and inversion symmetry simultaneously. Recently, we have found ferroelectricity induced by external fields in the one-dimensional CuO_2 ribbon chain oxide $Rb_2Cu_2Mo_3O_{12}$ without magnetic long range order.[18,19] We discussed the origin in terms of spin frustration between the nearest and next nearest neighbor spins,[20] and pointed out a possibility that a vector chiral order induced the ferroelectricity.

In this article we show the magnetoelectric effects in the pyrochlore-type oxide $Gd_2Ru_2O_7$ which is regarded as a three-dimensional frustrated spin system for the spins on the Gd ions. In this particular oxide, Gd^{3+} and Ru^{4+} ions are magnetic, and form a so-called pyrochlore lattice —a famous frustrated lattice in three dimension.[21] Although the spins on the Ru ions (the Ru spins) form a long range order below 113 K, the spins on the Gd ions (the Gd spins) do not show any trace of phase transition down to 2 K. A previous study has reported a jump due to the long-range order of the Ru spins at 113 K below which only a broad peak is seen around 5 K.[22] We find a finite magnetoelectric coupling in $Gd_2Ru_2O_7$, which mainly comes from the Gd spins without long range magnetic order. Comparing with $Gd_2Ti_2O_7$, we find that the coupling is one order of magnitude larger, and that the magnetic order of the Ru spins enhances the magnetoelectric effects. We propose a simple model for the Gd spins, and explain the observed values quantitatively.

2. Experimental

Polycrystalline samples of $Gd_2Ru_2O_7$ were prepared by a conventional solid-state reaction. A stoichiometric mixture of Gd_2O_3 and RuO_2 was ground and calcined at 850°C for 24 h and sintered at 1150°C for 48 h in air. For reference, polycrystalline samples of $Y_2Ru_2O_7$ and $Gd_2Ti_2O_7$ were also prepared. A stoichiometric mixture of Y_2O_3 and RuO_2 [Gd_2O_3 and TiO_2] was sintered at 1150°C [1350°C] for 48 h in air for $Y_2Ru_2O_7$ [$Gd_2Ti_2O_7$]. The x-ray diffraction measurements revealed that all the samples were in single phase.

The dielectric constant was measured with an ac capacitance bridge (Andeen Hagerling 2500A) at 1 kHz in a cryostat of Quantum Design PPMS in sweeping temperature from 2 to 15 K in a constant external field of 7 T, and in sweeping fields between 0 and 7 T at 5 K. The magnetization was measured with a SQUID magnetometer (Quantum Design MPMS) between 0 and 5 T at 5 K. Magnetrostriction was measured with a home-made setup using a strain gauge (KYOWA KFL-1-120-C1-11) in sweeping fields between 0 and 7 T at 5 K in the cryostat of Quantum Design PPMS.

3. Results and discussion

The dielectric constant $\varepsilon/\varepsilon_0$ of $Gd_2Ru_2O_7$ with and without an external field of 7 T is shown in the inset of Fig. 1. It shows a substantially large value of 15.2 at 15 K, and decreases with decreasing temperature. The large dielectric constant is also observed in the magnetoelectric Cr_2O_3 (11-13)[23] and the multiferroic $RMnO_3$ ($\sim$ 30).[24] Upon the applied field of 7 T,

*Present Address: Department of Physics, Faculty of Science and Technology, Tokyo University of Science, Noda 278-8510, Japan
†terra@cc.nagoya-u.ac.jp

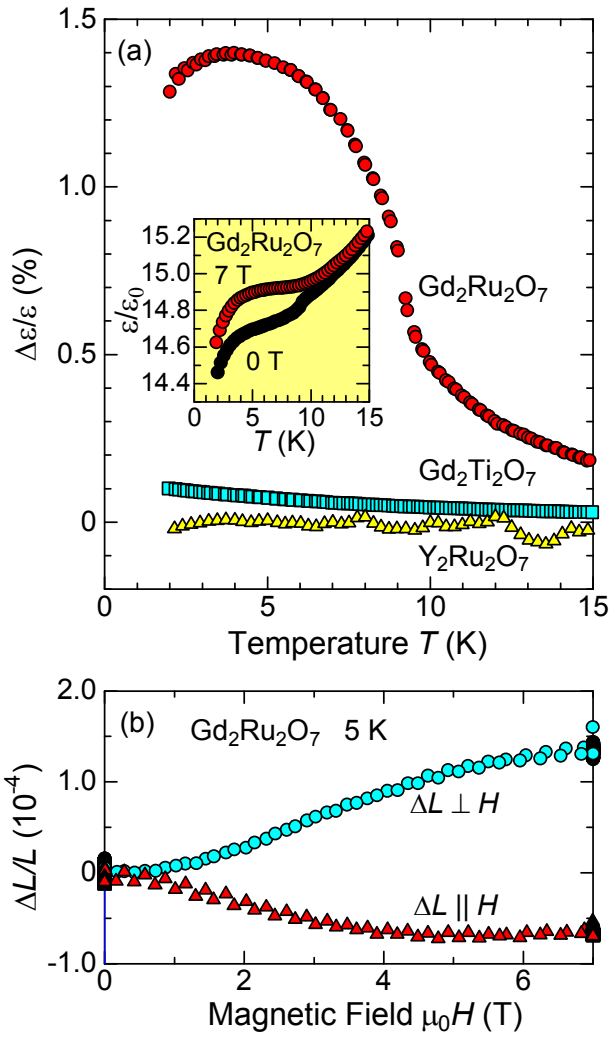

Fig. 1. (Color online) (a) The relative change in the dielectric constant induced by an external field of 7 T for $Gd_2Ru_2O_7$, $Y_2Ru_2O_7$ and $Gd_2Ti_2O_7$ plotted as a function of temperature. The inset shows the dielectric constant of $Gd_2Ru_2O_7$ plotted as a function of temperature with and without external field. (b) The magnetostriction $\Delta L/L$ of $Gd_2Ru_2O_7$ at 5 K.

it significantly increases below around 10 K. This clearly indicates a finite magnetoelectric coupling in this oxide. We do not fully understand the nature of the 10-K anomaly. A possible origin is that the Gd spins start to freeze below around this temperature.

Since $Gd_2Ru_2O_7$ has two kinds of magnetic ion of Gd^{3+} and Ru^{4+}, we experimentally specify which ion is responsible for the magnetoelectric coupling. Figure 1 shows the relative change in ε induced by the external field of 7 T defined by

$$\frac{\Delta\varepsilon}{\varepsilon} = \frac{\varepsilon(7\text{ T}) - \varepsilon(0\text{ T})}{\varepsilon(0\text{ T})} \tag{1}$$

for $Gd_2Ru_2O_7$, $Gd_2Ti_2O_7$ and $Y_2Ru_2O_7$. $\Delta\varepsilon/\varepsilon$ is largest in $Gd_2Ru_2O_7$, and essentially zero in $Y_2Ru_2O_7$. Thus the Gd spins are basically responsible for the magnetoelectric coupling. In $Gd_2Ru_2O_7$, the Ru spins are ordered in a non-collinear pattern possibly owing to the geometrical frustration. The Ru-Ru interaction is dominant, and determines the orientation of the Ru spins. Then the Gd spins align through the weaker Ru-Gd interaction. This situation is completely different from $Gd_2Ti_2O_7$ in which the frustration affects the ordering of the Gd spins through the Gd-Gd interaction. Since $\Delta\varepsilon/\varepsilon$ for $Gd_2Ti_2O_7$ is one order of magnitude smaller than that of $Gd_2Ru_2O_7$, thus we should take into account the magnetic order of the Ru spins which enhances the magnetoelectric coupling.

The magnetostriction is too small to explain the observed magnetoelectric effects. Figure 1(b) shows the magnetostriction of $Gd_2Ru_2O_7$ at 5 K plotted as a function of external field. The magnitude is of the order of 0.01 % at 7 T, which could only explain the 0.01% change in ε in Fig. 1(a). Thus we safely assume that the sample dimension is independent of external fields.

Before going into details, we will discuss here the spin structure of the Gd spins. Gurgul et al.[25] have reported that both the Ru spins and the Gd spins are ordered at 4.2 K. We carefully examined their work, and have come to the conclusion that the "order" of the Gd spins they called corresponds to an alignment of the Gd spins along the internal field from the Ru spins. We refer magnetic moments fully polarized by a strong external field as to "field-induced ferromagnetism" rather than "ferromagnetic order". The alignment of the Gd spins is such a case. The estimated ordered moment of the Gd spins remain only 10% of $J = 7/2$ near 80 K —well below T_N, and increases bending downwards with decreasing temperature.[?] This is what we expect in field-induced spin alignment. Also we emphasize that the jump of the specific heat is nearly identical between $Y_2Ru_2O_7$ and $Gd_2Ru_2O_7$, and the Gd spins make no substantial contribution to the phase transition around 113 K.[26] Thus Gd spins unlikely induce a spontaneous magnetization, and here we distinguish the Gd spin alignment from the Ru spin order.

We will seek for a simple model to explain the magnetoelectric effects. Figure 2 shows a schematic figure of the crystal structure of $Gd_2Ru_2O_7$, in which the Gd ions and the Ru ions form corner-shared tetrahedral clusters intervening with each other. Although all the Ru ions and all the Gd ions are equivalent, we will label numbers of 1–4 to specify the position relative to the Gd1 ion specified by the thick circle in the right figure of Fig. 2. First of all, considering the absence of long range order in the Gd spins, we neglect the magnetic interaction between the Gd spins. Thus the Hamiltonian that we seek for should describe a single Gd spin in external fields. Secondly, we take the magnetic order of the Ru spins into account. A previous neutron diffraction study has revealed that the Ru spins are ordered in a non-collinear structure,[27] in which the spins point to four different directions in a tetrahedron to satisfy

$$\boldsymbol{S}_{\text{Ru1}} + \boldsymbol{S}_{\text{Ru2}} + \boldsymbol{S}_{\text{Ru3}} + \boldsymbol{S}_{\text{Ru4}} = 0, \tag{2}$$

where $\boldsymbol{S}_{\text{Ru}i}$ is the spin on the site i in the Ru tetrahedron as is schematically shown in the left bottom figure in Fig. 2.

Let us introduce the magnetic interaction between the Gd1 spin and the neighboring Ru spins. As shown in Fig, 2, the Gd1 ion is surrounded with the six hexagonally-coordinated Ru ions of Ru2, Ru3 and Ru4 indicated by the solid lines. Then we write the Hamiltonian for Gd1 as

$$H_1 = -J(2\boldsymbol{S}_{\text{Ru2}} + 2\boldsymbol{S}_{\text{Ru3}} + 2\boldsymbol{S}_{\text{Ru4}}) \cdot \boldsymbol{S}_{\text{Gd1}}, \tag{3}$$

where J is the exchange energy between the i-th Ru spin $\boldsymbol{S}_{\text{Ru}i}$ and the Gd1 spin $\boldsymbol{S}_{\text{Gd1}}$. Using Eq. (2), we rewrite this Hamil-

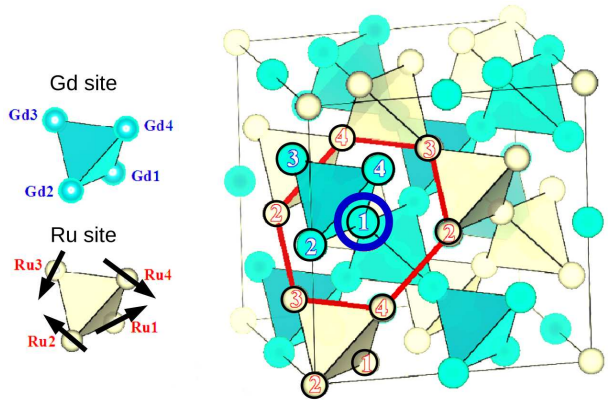

Fig. 2. (Color online) Crystal structure of $Gd_2Ru_2O_7$ (right) and the Gd tetrahedron and the Ru tetrahedron in the pyrochlore structure (left). The arrows on the Ru tetrahedron schematically indicate the directions of the ordered spin proposed from a neutron experiment.[27)]

tonian as

$$H_1 = 2J\boldsymbol{S}_{\mathrm{Ru1}} \cdot \boldsymbol{S}_{\mathrm{Gd1}}, \tag{4}$$

which means that H_1 is described only by the inner product of the Gd1 spin and the vector of $\boldsymbol{S}_{\mathrm{Ru1}}$. Note that $\boldsymbol{S}_{\mathrm{Ru1}}$ is introduced from Eq. (2), and no longer means the spin on the actual Ru1 site. Since the Ru spins have a long range order below 113 K, the magnetic interaction between the Ru spins is of the order of 100 K. Thus we assume that the direction of the Ru spin is independent of external field below 7 T at 5 K. By adding the Zeeman term of the external field $\mu_0\boldsymbol{H}$, we arrive at the Hamiltonian for the Gd1 ion as

$$H_1 = 2J\boldsymbol{S}_{\mathrm{Ru1}} \cdot \boldsymbol{S}_{\mathrm{Gd1}} - g\mu_{\mathrm{B}}\mu_0\boldsymbol{H} \cdot \boldsymbol{S}_{\mathrm{Gd1}}, \tag{5}$$

where g is the g factor and μ_{B} is the Bohr magneton.

In order to calculate various quantities, we replace the magnetic interaction from the Ru spins with a molecular field $\mu_0\boldsymbol{H}_{\mathrm{Ru}}$. Then the Hamiltonian of Gdi is finally written as

$$H_{\mathrm{mf}} = -g\mu_{\mathrm{B}}\mu_0(\boldsymbol{H}_{\mathrm{Ru}i} + \boldsymbol{H}) \cdot \boldsymbol{S}_{\mathrm{Gd}i}. \tag{6}$$

This Hamiltonian means that a spin on a Gd ion feels two different magnetic fields. In the absence of the external fields, the i-th Gd spin aligns parallel (or anti-parallel) to the i-th Ru spin, and thus the net moment $\boldsymbol{S}_{\mathrm{Gd1}}+\boldsymbol{S}_{\mathrm{Gd2}}+\boldsymbol{S}_{\mathrm{Gd3}}+\boldsymbol{S}_{\mathrm{Gd4}}$ is zero owing to Eq. (2), and the non-collinear arrangement identical to the Ru spins is gradually formed with decreasing temperature. In the presence of external fields, the Gd spins slightly cant to the field direction to induce a paramagnetic and linear magnetization. If the external fields were much larger than the molecular field, all the Gd spins would align parallel to the external field.

By using the Hamiltonian (6), we have numerically calculated the magnetization for each Gdi spin, and have obtained the bulk magnetization. To do so, we have taken a numerical average with respect to all the directions of the external field because the sample is a polycrystalline ceramics. To determine the magnitude of the molecular field μ_0H_{Ru}, we compare the calculation with various values of μ_0H_{Ru} with the measured magnetization. Figure 3(a) shows the magnetization plotted as a function of external field at 5 K. The calculated magnetization curves are also shown in Fig. 3(a), in which

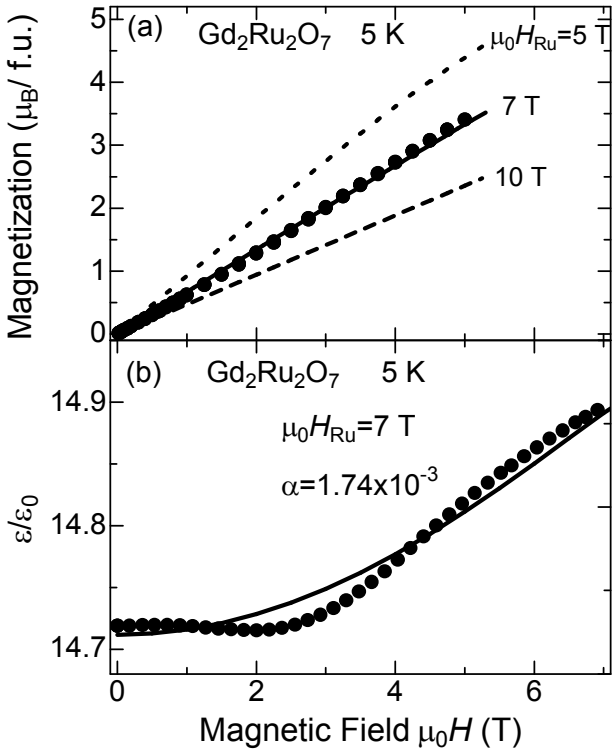

Fig. 3. (a) Magnetic field dependence of magnetization of $Gd_2Ru_2O_7$ at 5 K. The dotted, solid and dashed curves represent the calculation with μ_0H_{Ru} = 5, 7 and 10 T, respectively (For details, see text). (b) Magnetic field dependence of the dielectric constant of $Gd_2Ru_2O_7$ at 5 K. The solid curve represents the calculation with μ_0H_{Ru} = 7 T and $\alpha = 1.74\times10^{-3}$.

the values of μ_0H_{Ru} are indicated. Clearly, μ_0H_{Ru} = 7 T explains the measurement excellently. Considering that the full moment of Gd in formula unit is 14 μ_{B}, we find that 25% of the full moment observed at 5 T is reasonable with the value of μ_0H_{Ru} = 7 T.

Now let us discuss the magnetoelectric effect in $Gd_2Ru_2O_7$. Since the Gd spins show no long range order, the magnetoelectric effects observed here should have an origin different from those seen in Cr_2O_3 or $TbMnO_3$.[4,8)] Instead, similar magnetoelectric effects can be found in $EuTiO_3$[28)] and $BaMnF_4$,[29)] where the pair correlation of the spins plays a vital role. Katsufuji and Takagi[28)] have proposed that the dielectric constant of $EuTiO_3$ is described by

$$\varepsilon(T,H) = \varepsilon(T,0)(1 + \alpha\langle\boldsymbol{S}_i \cdot \boldsymbol{S}_j\rangle), \tag{7}$$

where $\boldsymbol{S}_i$ is the spin on the Eu ion at the i site, and α is the magnetoelectric coupling constant. They have also discussed the dielectric constant of $Gd_2Ti_2O_7$ in a similar way.[30)]

Following Katsufuji and Takagi, let us calculate the dielectric constant of $Gd_2Ru_2O_7$. Since we have already calculated the average of the Gd spins $\langle\boldsymbol{S}_i\rangle$ at 5 K with μ_0H_{Ru} = 7 T, we approximate $\langle\boldsymbol{S}_i \cdot \boldsymbol{S}_j\rangle$ by taking the inner product of $\langle\boldsymbol{S}_i\rangle$ and $\langle\boldsymbol{S}_j\rangle$ where i and j are taken with respect to the nearest neighbor Gd sites.

Figure 3(b) shows the dielectric constant $\varepsilon/\varepsilon_0$ at 5 K plotted as a function of external field. $\varepsilon/\varepsilon_0$ shows a non-monotonic change with magnetic field; it is essentially constant below 2 T, whereas it increases linearly with larger external fields. We also plot the calculation based on Eq. (7) by the solid curve, where μ_0H_{Ru} = 7 T and $\alpha = 1.74\times10^{-3}$. In the absence of ex-

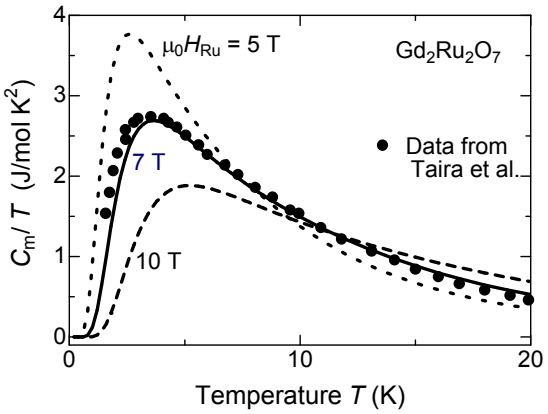

Fig. 4. Magnetic specific heat C_m divided by temperature T of $Gd_2Ru_2O_7$. The experimental data represented by solid circles are taken from Taira et al.[22] The dotted, solid and dashed curves represent the calculation with $\mu_0 H_{Ru}$ = 5, 7 and 10 T, respectively (For details, see text).

ternal field, the Gd spins have the non-collinear arrangement to have $\langle \boldsymbol{S}_i \cdot \boldsymbol{S}_j \rangle = 0$. With increasing external field, the Zeeman term starts to cant the Gd spins parallel to the field against the molecular filed of 7 T, and give finite values of $\langle \boldsymbol{S}_i \cdot \boldsymbol{S}_j \rangle$. This effect is roughly quadratic with external field, and becomes significant when $H \sim H_{Ru}$. We find that the calculation explains the measured magneto-dielectric constant fairly well. The fitting is consistent with the previous work in $EuTiO_3$ in the sense that the obtained α is close to α (= 2.74×10^{-3}) of $EuTiO_3$.[28]

In order to further examine the validity of Eq. (6), we compare the specific heat data with the Shottkey specific heat of $S = 7/2$ with the internal field. In Fig. 4, the magnetic part of the specific heat C_m divided by temperature T reported by Taira et al.[22] is shown by the closed circles. The dotted, solid and dashed curves represent the calculation based on Eq. (6) with values of $\mu_0 H_{Ru}$ = 5, 7 and 10 T, respectively. The curve for $\mu_0 H_{Ru}$ = 7 T explains the measured data excellently, and we have come to the conclusion that Eq. (6) with $\mu_0 H_{Ru}$ = 7 T quantitatively explains the thermodynamic quantities of $Gd_2Ru_2O_7$ at low temperatures.

In our work, we have only assumed the Gd-Ru interaction with the ordered structure of the Ru spins for the sake of simplicity. If we took the Gd-Gd interaction into account, the experimental data at low temperatures would be better described. To do so, we have to introduce more free parameters, and the reliability of the fitting will go worse. Such studies should be done in a next stage to see the dependence on magnetic-field orientation using single crystals.

4. Summary

We have prepared polycrystalline samples of $Gd_2Ru_2O_7$, $Y_2Ru_2O_7$ and $Gd_2Ti_2O_7$, and have investigated their magnetoelectric effects. We have found that a substantial magnetoelectric coupling in $Gd_2Ru_2O_7$, which arises from the interaction between the Gd spins and the Ru spins. We have proposed a simple model and have calculated the magnetization and specific heat, which are in excellent agreement with the experimental results. The same model has also explained the field dependence of the dielectric constant of $Gd_2Ru_2O_7$. We conclude that the magneto-dielectric constant of $Gd_2Ru_2O_7$ comes from the pair correlation of the Gd ions with the internal field of 7 T from the Ru spin clusters. We have evaluated the magnetoelectric coupling constant α to be 1.74×10^{-3}, which is comparable to α in $EuTiO_3$.

Acknowledgment

This study was supported by a Grant-in-Aid for Scientific Research on Priority Areas “Novel States of Matter Induced by Frustration” (Kakenhi No.22014005).

1) E. Bertaut and M. Mercier: Mater. Res. Bull. **6** (1971) 907 .
2) M. Fiebig: J. Phys. D **38** (2005) R123.
3) W. Eerenstein, N. D. Mathur, and J. F. Scott: Nature **442** (2006) 759.
4) D. N. Astrov: Soviet Phys.-JETP **11** (1960) 708.
5) V. J. Folen, G. T. Rado, and E. W. Stalder: Phys. Rev. Lett. **6** (1961) 607.
6) G. T. Rado and V. J. Folen: Phys. Rev. Lett. **7** (1961) 310.
7) H. B. Lal, R. Srivastava, and K. G. Srivastava: Phys. Rev. **154** (1967) 505.
8) T. Kimura: Ann. Rev. Mater. Res. **37** (2007) 387.
9) S.-W. Cheong and M. Mostovoy: Nat. Mater. **6** (2007) 13.
10) J. F. Scott and R. Blinc: J. Phys.: Condens. Matter **23** (2011) 113202.
11) T. Choi, Y. Horibe, H. T. Yi, Y. J. Choi, W. Wu, and S.-W. Cheong: Nat. Mater. **9** (2010) 253.
12) S. Seki, X. Z. Yu, S. Ishiwata, and Y. Tokura: Science **336** (2012) 198.
13) T. Zhao, A. Scholl, F. Zavaliche, K. Lee, M. Barry, A. Doran, M. P. Cruz, Y. H. Chu, C. Ederer, N. A. Spaldin, R. R. Das, D. M. Kim, S. H. Baek, C. B. Eom, and R. Ramesh: Nat. Mater. **5** (2006) 823.
14) J. Ma, J. Hu, Z. Li, and C.-W. Nan: Adv. Mater. **23** (2011) 1062.
15) Y. Yasui, M. Sato, and I. Terasaki: J. Phys. Soc. Jpn. **80** (2011) 033707.
16) Y. Yasui, Y. Yanagisawa, M. Sato, and I. Terasaki: J. Phys.: Conf. Ser. **320** (2011) 012087.
17) S. Kori, T. Okamura, R. Okazaki, I. Terasaki, and Y. Yasui: Phys. Rev. B **91** (2015) 144403.
18) Y. Yasui, Y. Yanagisawa, R. Okazaki, I. Terasaki, Y. Yamaguchi, and T. Kimura: J. Appl. Phys. **113** (2013) 17D910.
19) Y. Yasui, Y. Yanagisawa, R. Okazaki, and I. Terasaki: Phys. Rev. B **87** (2013) 054411.
20) Y. Yasui, R. Okazaki, I. Terasaki, M. Hase, M. Hagihala, T. Masuda, and T. Sakakibara: JPS Conf. Proc. **3** (2014) 014014.
21) J. S. Gardner, M. J. P. Gingras, and J. E. Greedan: Rev. Mod. Phys. **82** (2010) 53.
22) N. Taira, M. Wakeshima, and Y. Hinatsu: J. Mater. Chem. **12** (2002) 1475.
23) P. H. Fang and W. S. Brower: Phys. Rev. **129** (1963) 1561.
24) T. Kimura, G. Lawes, T. Goto, Y. Tokura, and A. P. Ramirez: Phys. Rev. B **71** (2005) 224425.
25) J. Gurgul, M. Rams, Z. Swiatkowska, R. Kimec, and K. Tomala: Phys. Rev. B **75** (2007) 064426.
26) M. Ito, Y. Yasui, M. Kanada, H. Harashina, S. Yoshii, K. Murata, M. Sato, H. Okumura, and K. Kakurai: J. Phys. Chem. Solids **62** (2001) 337 .
27) M. Ito, Y. Yasui, M. Kanada, H. Harashina, S. Yoshii, K. Murata, M. Sato, H. Okumura, and K. Kakurai: J. Phys. Soc. Jpn. **69** (2000) 888.
28) T. Katsufuji and H. Takagi: Phys. Rev. B **64** (2001) 054415.
29) J. F. Scott: Phys. Rev. B **16** (1977) 2329.
30) T. Katsufuji and H. Takagi: Phys. Rev. B **69** (2004) 064422.